PAPER

Cu²⁺ recognition by *N,N'*-benzylated bis(amino amides)†

Lingaraju Gorla, Vicente Martí-Centelles, Belén Altava,* M. Isabel Burguete and Santiago V. Luis*

Two new C_2-symmetric *N,N'*-benzylated bis(amino amides) have been synthesised and their interaction with different transition metals studied using a variety of techniques including UV-Vis and CD spectroscopy or ESI-MS. The determination of the corresponding stability constants with Cu²⁺ has been possible, in H_2O/CH_3CN 7/3 v/v, for one of these ligands (**4**) using potentiometric titrations. The results obtained reveal that *N*-benzylation affords significant changes to their properties and is accompanied by an appreciable decrease in the corresponding complexation stability constants. However, this, along with the low kinetics associated to Ni²⁺, facilitates the recognition of Cu²⁺ by **4** that can be followed by the naked-eye up to the submillimolar range. Very interestingly, the chiral nature of this ligand provides an intense and well defined CD curve for the corresponding Cu²⁺ complex, very sensitive to the coordination geometry, facilitating the analysis of this interaction even at the µM range. The formation by both ligands (**3** and **4**) of square planar complexes with Cu²⁺ and Ni²⁺ displaying a 1 : 1 stoichiometry was confirmed by their X-ray crystal structures.

Introduction

The design, preparation and study of organic ligands able to interact with specific transition metals are of great current interest for the relevant role of these metals in different areas of chemistry and biology. These ligands can be useful for the selective extraction, removal or sensing of biologically and environmentally important species.[1] Transition metals are not only required for biological functions but also have great potential for industrial applications. Among the various transition metal ions, Cu²⁺ plays important roles in living systems as a nutrient trace element present in the active sites of some key enzymes, but, at the same time, it is also associated with some serious human physiological dysfunctions such as Alzheimer's and Prion type neurodegenerative diseases, amyotrophic lateral sclerosis, Wilson's disease *etc*.[2] The selective interaction with Cu²⁺ has allowed the development of sensing systems through the quantification of photophysical signals,[3] including molecular probes providing logistics of naked-eye detection through a colour change for visual perception.[3e,4]

In this regard, nitrogen binding sites are commonly used as donor atoms for ligand design,[5] and different amino acid derivatives have been shown to bind metals forming stable complexes and the results are of interest to understand the interaction of proteic structures with metals.[6] Recent contributions from our group have revealed that C_2-symmetrical bis(amino amides) derived from amino acids form stable complexes with Cu²⁺, Zn²⁺ and Ni²⁺ ions.[7] These results have highlighted the importance of different structural factors for this interaction and suggested that the presence of aromatic rings at different positions can be a key structural element. In particular, the inclusion of benzyl and related groups can be very relevant for the properties of the resulting ligands as has been reported for catalytic applications,[6a–c] and more recently in cascade-systems for the recognition of dicarboxylates.[8] Herein, we present the synthesis of two new open-chain *N,N'*-benzylated bis(amino amide) ligands derived from ʟ-phenylalanine (**3**) and ʟ-valine (**4**) and the study of their acid–base properties as well as their metal complexation capacity, in particular for Ni²⁺ and Cu²⁺ using a variety of techniques.

Results and discussion

Synthesis, characterization and acid–base properties of the ligands

Scheme 1 displays the general synthetic pathway for the preparation of ligands **3** and **4**. Bis(amino amides) **1** and **2**, derived

Departamento de Química Inorgánica y Orgánica, Universitat Jaume I, Avda. Sos Baynat s/n., 12071 Castellón, Spain. E-mail: altava@uji.es, luiss@uji.es; Fax: +34 964728214; Tel: +34 964728239
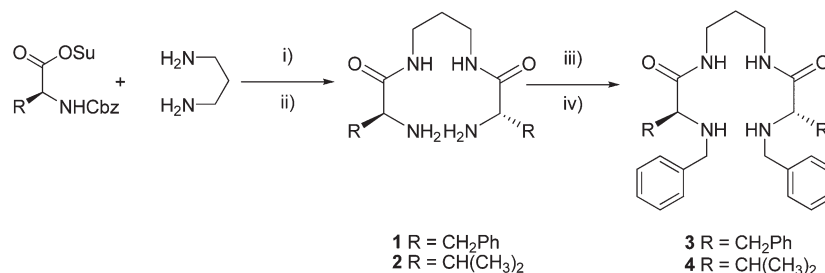
Scheme 1 Synthesis of ligands **3** and **4**. (i) DME, 20 h, r.t., 70–80%; (ii) HBr/AcOH 8 h, NaOH, r.t., 60–70%; (iii) benzaldehyde, methanol, 2 h, r.t; (iv) sodium borohydride, 18 h, r.t., 70–80%.

from L-phenylalanine and L-valine, were prepared from the corresponding N-Cbz protected amino acid N-hydroxysuccinimide ester, via coupling with 1,3-diaminopropane and final N-deprotection using HBr/AcOH.[9] Then, compounds **1** and **2** were subjected to a reductive amination process, using benzaldehyde in methanol and then sodium borohydride, to afford ligands **3** and **4** in good yields.[10] A central spacer containing three methylene groups was selected as previous results had shown that this spacer is very well suited to favour the formation of strong 1 : 1 metal complexes with the bisdeprotonated ligand.[7a,b]

Ligands **3** and **4** were fully characterised using standard techniques (¹H-NMR, ¹³C-NMR, ESI-MS, and FT-IR), and crystals suitable for single-crystal X-ray diffraction analysis were obtained in the case of **3**.

The crystal lattice for **3** (ESI, Fig. S1†) highlights the potential of this ligand to self-associate through well-defined directional supramolecular interactions and the importance of the aromatic rings in this regard. Interestingly, one of the benzyl side chains is folded over the central spacer in such a way that all the nitrogen bound hydrogen atoms are located at relatively short distances of this aromatic ring (<4.2 Å for the shortest N–H⋯C_{Ar} distance) in particular for one of the amino groups (2.906 Å). The importance of the interactions N–H⋯Ar in peptide-like molecules has been highlighted in several examples of pseudopedtidic minimalistic molecular rotors.[11] The most prominent feature for the crystal organization is that a defined set of H-bonds induces a global parallel disposition of the molecules (a β-sheet-like arrangement) with carbonyl groups from the two amides of each molecule located in anti-position (Fig. 1), and H-bonding to the amide groups of two additional molecules located at the two opposite sites. A

different pattern was observed for the analogous compound with a shorter aliphatic spacer, displaying a syn disposition of the carbonyl amide groups and both aromatic side chains oriented in opposite directions.[8]

The proper determination of the acid–base properties of polyamines is essential for understanding their coordination properties.[12,13] The protonation constants of bis(amino amides) **3** and **4** were determined by potentiometric titrations. The presence of CH_3CN as co-solvent was required to guarantee the solubility of the ligands and all the titrations were carried out at 298.1 K, using 0.1 M NaCl in H_2O/CH_3CN 7/3 v/v to maintain a constant ionic strength. The obtained stepwise stability constants for the protonation of pseudopeptidic ligands **3** and **4**, using the program HYPERQUAD,[14] are presented in Table 1. For the potentiometric studies in this solvent mixture, K_w was determined to be 14.6 in good agreement with literature data.[15] The starting bis(amino amides) **1** and **2** had been studied previously in 0.15 or 0.10 M NaCl.[7a,b] To facilitate a proper comparison, the acid–base properties of **2** in 0.1 M NaCl in H_2O/CH_3CN 7/3 v/v were also determined.

As expected, the double N-benzyl substitution decreased the basicity of the resulting bis(amino amides), (i.e. $\log K_{H1}$ 7.77 for **2** against $\log K_{H1}$ 6.74 for **4**). Regarding the effect of the amino acid residue, the values of the first protonation constants for **3** ($\log K_{H1}$ 6.77) and **4** ($\log K_{H1}$ 6.74) were very close, while for the second protonation constant the value obtained for **3** ($\log K_{H2}$ 5.15) was more than one order of magnitude lower than the one for **4** ($\log K_{H2}$ 6.73) (Table 1). The similar values for the two protonation constants of **4** are remarkable. In α,ω-alkyldiamines, the difference between the two protonation constants decreases with the length of the spacer as a consequence of the reduction in the electrostatic repulsion
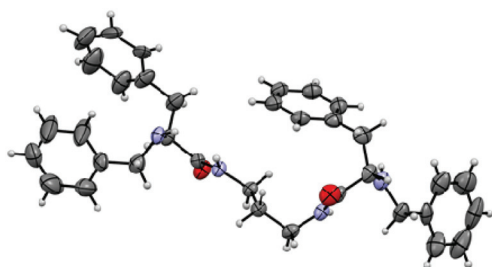

Fig. 1 X-ray crystal structure of ligand **3**.

Table 1 Logarithms of the stepwise basicity constants of ligands **1**–**4** determined at 298.1 ± 0.1 K[b]

| Reaction[a]	**1**[c,f]	**2**[d,g]	**2**[e]	**3**[e]	**4**[e]
H + L ⇌ HL	7.57(1)	8.01(5)	7.77(8)	6.77(7)	6.74(9)
H + HL ⇌ H₂L	6.70(1)	6.96(7)	7.11(8)	5.15(1)	6.73(9)

[a] Charges omitted for clarity. [b] Values in parentheses are the standard deviations in the last significant figure. [c] Determined in 0.1 M NaCl. [d] Determined in 0.15 M NaCl. [e] 0.1 M NaCl in H_2O/CH_3CN 7/3 v/v. [f] Data taken from ref. 7b. [g] Data taken from ref. 7a.

between the two protonated sites, but remains essentially constant after pentamethylenediamine ($\Delta \log K \approx 0.9$), which has been associated to statistical factors.[12b] The situation, however, is more complex when additional heteroatoms or functional groups are present as has been observed for large polyamines and polyazacycloalkanes.[12b,16] Thus, for 1,5,9,13,17,21-hexaazaheneicosane containing propylenic spacers, identical $\log K$ values have been reported for the first two protonation steps.[16a] The same situation was observed for the macrocycle [32]aneN$_6$ displaying two 1,5,9-triazanonane subunits separated by two heptamethylene chains.[16b,c] Very close constants have also been found for the two first protonation constants ($\Delta \log K \leq 0.2$) in [24]aneN$_6$,[16d] [27]aneN$_9$,[16e] and [36]aneN$_{12}$.[16f] These results cannot be only explained by the changes in the statistical factors associated to large polyamines and hydrogen bonding and entropic contributions have to be considered. A similar situation had been previously observed, always in mixed solvents, in a few C_2-symmetric pseudopeptides,[7d,17] Solvent effects are important on protonation constants and in the case of some polyamines it has been shown that these effects can differ for the first and the second protonation steps.[18] For one of the pseudopeptides previously studied, changing the solvent provided a strong reduction of the first protonation constant ($\Delta \log K = -1.04$) while the second one slightly increased ($\Delta \log K = 0.19$).[7d] The comparison of the protonation constants for the reference compound 2 in the two solvent systems in Table 1 reveals a related trend, suggesting that the same can apply here. This could reflect the involvement of the amino groups in strong hydrogen bonding in the non-protonated compound that has to be broken for the first protonation to occur. The importance of intramolecular hydrogen bonds in diamides,[19] the role of aromatic fragments on the solvation and hydrogen bonding in pseudopeptidic structures,[11] and the resulting effects on the acid–base properties of the groups involved,[19b] have been studied in detail. Overall the situation is reminiscent of the one found in polytopic systems displaying positive cooperativity,[20] in particular ditopic allosteric systems for which binding of the first guest requires a reorganization of the whole system that facilitates the binding of the second guest.[21] A relevant example is a tetramide-crown ether system in which hydrogen bonding inhibits anion binding that is then "switched on" through an initial cation complexation.[22] The distribution diagrams (ESI, Fig. S2†) revealed the presence of H$_2$L^{2+} as the predominant species at pH values lower than 5 and 4 for ligands 3 and 4 respectively while the neutral species were predominant for both ligands at pH > 8. The most relevant difference is related to the monoprotonated species HL. The lower value of the second protonation constant for 3 is reflected in the presence of HL as a more important species at pH values close to neutrality, being the major species at pH 6.

Interaction of ligands 3 and 4 with M^{2+} species

Synthesis and characterization of Cu^{2+} and Ni^{2+} complexes.
The corresponding Cu^{2+} and Ni^{2+} complexes derived from ligands 3 and 4 were synthesised in basic MeOH (Scheme 2)
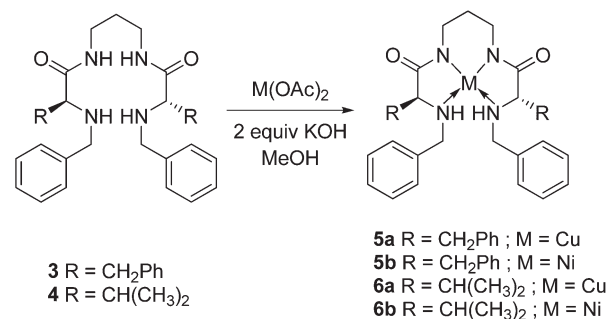
Scheme 2 Synthesis of the metal complexes derived from bis(amino amides) 3 and 4.

allowing the generation of the neutral metal complexes 5 and 6. This was evidenced by the change of colour from blue to orange for the copper complexes 5a and 6a and from green to maroon for the nickel complexes 5b and 6b. Moreover, the formation of the complexes could be followed by FT-IR through the significant shift of the C=O band to lower frequencies when the complexes were formed (i.e. 1551 cm^{-1} for 6a against 1629 cm^{-1} for 4, ESI, Fig. S3†) indicative of the deprotonation of the N–H amide groups.[6h]

UV-Vis and CD studies. The higher solubility of the metal complexes from ligand 4 in polar protic solvents allowed the corresponding spectroscopic studies in MeOH/H$_2$O 80/20 v/v. No significant differences were observed for the UV-Vis spectra of the copper complexes of 4 in this solvent and in H$_2$O/CH$_3$CN (7/3 v/v). Initially, 1.2 equivalents of ligand 4 were added (200 μL of a 30 mM solution, MeOH/H$_2$O 80/20 v/v) to a set of vials containing the acetate salts for Cu^{2+}, Zn^{2+}, Ni^{2+} and the chloride salts for Co^{2+} and Cd^{2+} in the same solvent (2.5 mM, 2 mL) and the corresponding UV-Vis spectra were analysed (ESI, Fig. S4†). The pH of all the solutions was close to neutrality and the addition of the ligand only afforded slight pH changes (ESI, Table S2†). For Cu^{2+}, an intense peak at 490 nm and a small one at 750 nm were observed, along with a purple colour in the solution. For Ni^{2+}, two small absorption peaks at 400 and 650 nm were present. Only a very weak absorption at 500 nm was observed for Co^{2+}.[23] As expected, no absorption peaks between 400 to 800 nm were observed for Zn^{2+} and Cd^{2+} and the resulting solutions remained colourless (ESI, Fig. S4†).

For the Cu^{2+}·4 system a large increase was observed on the molar absorption coefficients for the bands of the ligand at low wavelengths, characteristic of charge-transfer processes when large interactions between the molecular orbitals of the ligand and those of the metal occur.[23] Besides, the two absorption peaks at 490 nm 750 nm suggest the coexistence of two coordination geometries for the metal, probably square planar and octahedral respectively.[24] For the Ni^{2+}·4 system, the initial absorption peaks observed around 400 and 650 nm suggested an octahedral structure,[25] but when the UV-Vis spectrum was again measured after 24 hours, a new peak at 460 nm, usually associated to square planar Ni^{2+} complexes,[26] was detected in

agreement with the slow kinetics associated to this metal cation (ESI Fig. S4†).[27] For Co^{2+}, the small absorption at 500 nm suggests the occurrence of an octahedral structure.[25a]

Upon addition of *ca.* 2 equiv. of a 0.1 M NaOH solution in water to these $M^{2+} \cdot 4$ systems (*ca.* 2.3 mM in the metal), pH values of 9.1–9.8 were obtained (ESI, Table S2†) and for Cu^{2+} the color became more intense. For this system, the UV-Vis (ESI, Fig. S4†) showed the disappearance of the band at 750 nm and the increase in the intensity of the absorption at 490 nm ($\varepsilon = 123$ M^{-1} cm^{-1}) suggesting the quantitative formation of a square planar complex (ESI Fig. S4 and S5†). The stoichiometry of the complex formed by **4** and Cu^{2+} was determined to be 1 : 1 (ligand : metal) from the Job plot of its absorbance at 490 nm as a function of the molar fraction of added Cu^{2+} in MeOH/H_2O (ESI, Fig. S6†).[28,29] The titration of Cu^{2+} solutions with increasing amounts of **4** provided a gradual increase in the intensity of the absorption at 490 nm and a decrease of the one at 750 nm. The isoemissive point around 640 nm was better defined under basic conditions. The non-linear fitting of the titration curves (1 : 1 stoichiometry) provided apparent constants (K_{app}) of 562 M^{-1} and 3350 M^{-1} in the absence and presence of base (ESI, Fig. S7†).[28] Similar trends were obtained when $CuCl_2$ and $CuNO_3$ were used instead of $Cu(OAc)_2$ as the source of Cu^{2+} (ESI, Fig. S8†).

Considering the chiral nature of the ligand, the complexation of **4** with the different metal ions was also studied by CD. For this purpose, a 2.5 mM solution (MeOH/H_2O 80/20 v/v) containing an equimolecular mixture of **4** and the corresponding M^{2+} and two equivalents of base was kept stirring for 24 hours. The CD of the free ligand **4** displayed a negative band centered at 240 nm (Fig. 2a). Very interestingly, in the presence Cu^{2+} (Fig. 2b, black line) a strong negative split-Cotton effect (−, +) was observed with a minimum at 529 nm ($\Delta\varepsilon = -0.44$ cm^2 mol^{-1}) and a maximum at 448 nm ($\Delta\varepsilon = 0.23$ cm^2 mol^{-1}), and passing through zero at 481 nm, which is the λ_{max} for the UV band for the square planar complex. In the absence of added base, an additional weaker positive CD band was observed for the $Cu^{2+} \cdot 4$ system in the 600–800 nm region (ESI, Fig. S13†) in agreement with the coexistence of

two complex species and highlighting the very different 3D chiral environments present in them. This behaviour was not detected for other metals. Only for Ni^{2+}, a weak Cotton effect (minimum at 463 nm, maximum at 284 nm) was observed (Fig. 2b). Additional CD signals were always observed below 350 nm most likely related to metal–ligand charge transfer or to intraligand transitions.[23,30]

Taking into account that most molecular designs for the detection of Cu^{2+} involve the inclusion of sensitive chromogenic or fluorescent units like Rhodamine, naphthalimide, squarylium, fluorescein, *etc.*,[3,4,31] the optical response obtained for $Cu^{2+} \cdot 4$ complexes, in particular in CD, is remarkable. Nevertheless, the approximated LOD value calculated for the naked-eye detection was *ca.* 0.25 mM (ESI, Fig. S9†),[32] while the use of UV-Vis spectra provided LOD values in the 79–91 µM range, depending on the experimental conditions (ESI, Fig. S10 to S12†). Although the naked-eye detection can compare well with some reported sensors (µM–mM range in many cases), the UV-Vis LOD values are significantly higher than those in sensors containing chromogenic fragments.[31] It is worth noting that the strong CD Cotton effect observed allowed to obtain lower LOD values of 43 µM and 28 µM under neutral and basic conditions respectively by using the variation of the amplitude of the Cotton effect ($\Delta CD = CD_{440nm} - CD_{520nm}$) (ESI, Fig. S13 and S14†),[33] no interference by the other metals assayed was observed in any of the cases (ESI, Fig. S15†).

ESI-MS studies for the metal complexes. ESI-MS experiments with ligand **4** supported its preferential binding to Cu^{2+}. The ESI^+-MS in the presence of 1 equiv. of $Cu(AcO)_2$, displayed peaks at 514.4 and at 574.3, the latter being the base peak, associated to $[CuH_{-2}L + H]^+$ and $[CuH_{-2}L + H + AcOH]^+$ or to $[CuH_{-1}L]^+$ and $[CuH_{-1}L + AcOH]^+$ and supporting a 1 : 1 complexation (Fig. 3). For Ni^{2+}, Cd^{2+}, Co^{2+}, Zn^{2+} ions, the corresponding peaks associated to $[MH_{-1}L]^+$ species were not observed, although the peak for the $[MH_{-1}L + AcOH]^+$ species was present for Zn^{2+} and Ni^{2+}. However, for Ni^{2+}, the intensity of this peak was 30% of the base peak while for Zn^{2+} its intensity was <2% (ESI, Fig. S16†). For Co^{2+} and Cd^{2+} very minor peaks (<2%) corresponding to $[2L + M]^{2+}$ and $[L + M + Cl]^+$ species were observed.

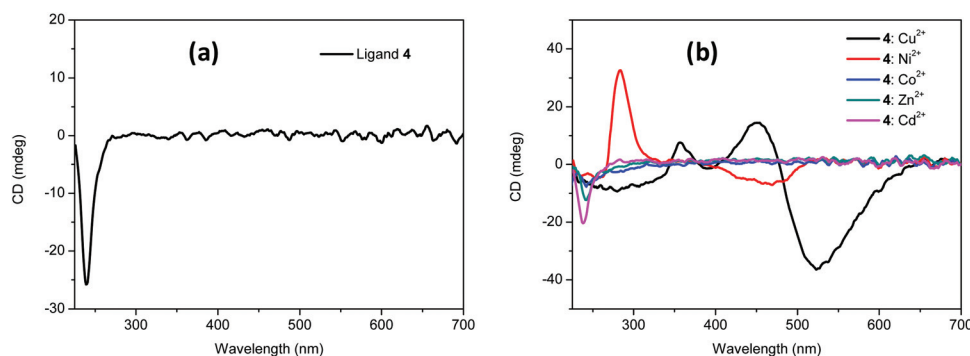**Fig. 2** (a) CD spectra for ligand **4** in basic media (2 equiv. of NaOH). (b) CD spectra for ligand **4** in basic media (2 equiv. of NaOH) in the presence of 1 equivalent of different M^{2+} metals. In all cases the solvent was MeOH/H_2O 80/20 (v/v) and the concentration of the metal and the ligand 2.5 mM.
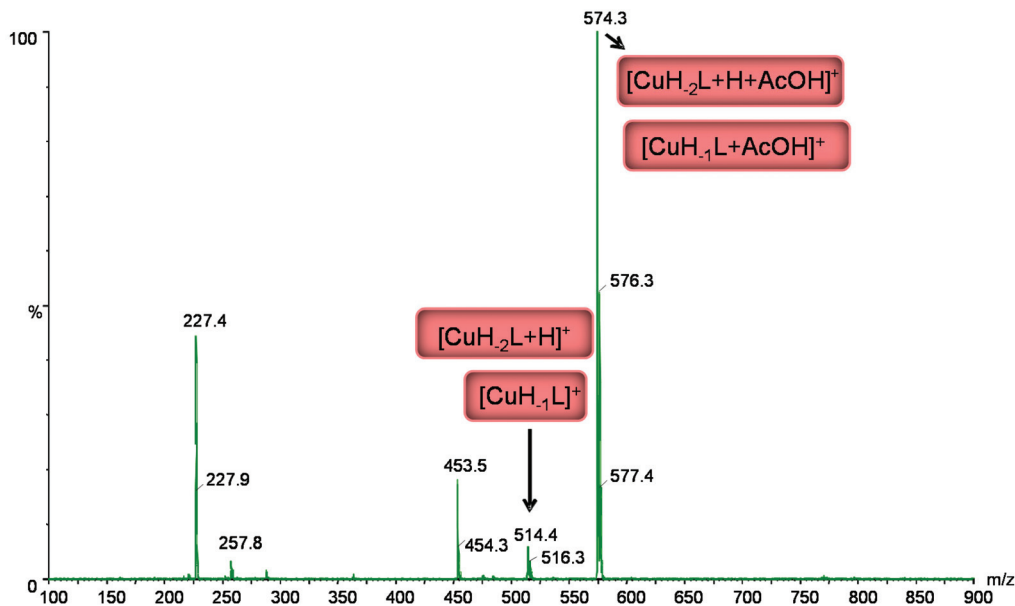
Fig. 3 ESI⁺-MS of compound **4** (5 mM) in the presence of 1 equiv. of Cu(OAc)₂ in MeOH/H₂O 80/20, v/v.

Potentiometric studies for Cu²⁺ complexes

Finally, the interaction of ligand **4** with Cu^{2+} was studied by potentiometric titrations over the 2–12 pH range. The stability constants for the formation of complexes were determined for a 1 : 1 metal–ligand ratio, using NaCl 0.1 M in H_2O/CH_3CN 7/3 v/v to maintain a constant ionic strength and at 298.1 K. Although the same solvent mixture used for spectroscopic measurements was also assayed here (MeOH/H₂O 80/20 v/v), its use was not satisfactory and led to non-stable measurements in some instances. The results obtained are presented in Table 2 and the corresponding distribution diagrams are displayed in Fig. S17 (ESI†). The interaction of the starting bis(amino amide) **2** with Cu^{2+} was also studied by potentiometric titrations using the same medium to provide a proper comparison. The solubility problems associated to ligand **3** complexes again precluded carrying out accurate potentiometric titrations. When comparing the values obtained for **2** in both solvents it can be seen that the solvent plays, in this case, an important role. The formation of complex species seems to be favoured in the mixed solvent,[7a] although the effects coming from the stronger competition of Na⁺ in the medium of greater salinity need to be also considered.

As can be seen in Table 2, significant differences can be observed associated to the *N*-benzylation. The most general and remarkable observation was the lower stability of the non-deprotonated, mono and di-deprotonated complex species for compound **4**. This is easily analysed using the representation of the $\log K_{\text{eff}}$ values *vs.* pH (Fig. 4). For the neutral [CuH₋₂L] species from **4** the formation constant ($\log \beta = -6.29$) was more than three orders of magnitude lower than the related one for ligand **2** ($\log \beta = -2.97$). In spite of this, these neutral complex species were predominant around pH 7 for **2** and **4**, though [CuH₋₂L] starts to be formed at slightly higher pH values for **4**. This confirms the formation of [CuH₋₂L] species at physiologic pH for **4** (ESI, Fig. S17†). On the other hand, the relative importance of [CuH₋₁L] and [CuL] species is reversed for both ligands. For **4**, the [CuH₋₁L] species is more important at pH values around 6, while it is a minor species in the case of **2**, and [CuL] is relatively important for **2** at pH values
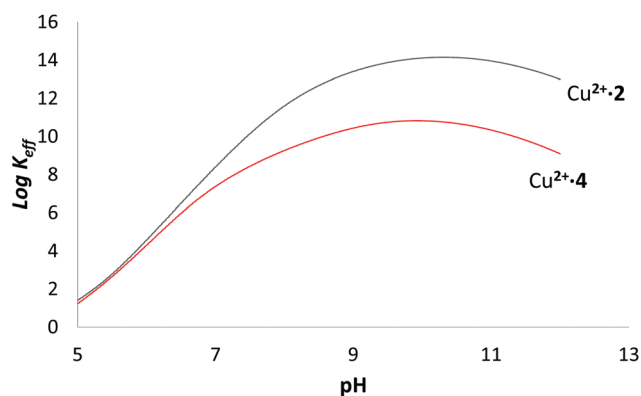
Table 2 Logarithms of the formation constants ($\log \beta$) for the Cu²⁺ complexes with ligands **2** and **4** at 298.1 ± 0.1 K[b]

Reaction[a]	**2**[c,d]	**2**[e]	**4**[e]
Cu + L ⇌ CuL	5.99(3)	6.99(7)	4.39(9)
Cu + L ⇌ CuH₋₁L + H	0.53(1)	1.53(7)	−0.66(3)
Cu + L ⇌ CuH₋₂L + 2H	−6.66(1)	−2.97(1)	−6.29(1)

[a] Charges omitted for clarity. [b] Values in parentheses are the standard deviations in the last significant figure. [c] Determined in 0.15 M NaCl. [d] Data taken from ref. 7a. [e] 0.1 M NaCl in H₂O/CH₃CN 7/3 v/v.

Fig. 4 Plot of the effective conditional constants *vs.* pH for the systems Cu²⁺·**2** and Cu²⁺·**4** in 0.1 M NaCl in H₂O/CH₃CN 7/3 v/v, at 298.1 ± 0.1 K.

close to **5**, whereas it is very minor for **4**. The distribution diagram obtained for **4** reveals that at neutral pH values at least two species are present, [CuH$_{-2}$L] and [CuH$_{-1}$L], which is in good agreement with the observations obtained from spectroscopic experiments suggesting the coexistence of square planar and octahedral Cu^{2+} species. The decrease observed in the stability of the Cu^{2+} complexes upon benzylation of the terminal amino groups of **2** is higher than that observed for the benzylation of some linear polyamines, where the magnitudes of the stability constants were 1–2 orders of magnitude lower,[23c] although for a triethylenetetramine bearing anthracene and benzophenone instead of phenyl units an additional decrease in *ca.* five logarithmic units has been reported.[13g]

Single-crystal X-ray diffraction studies

The formation of the corresponding bisdeprotonated complexes of **3** and **4** with Cu^{2+} and Ni^{2+} and their stoichiometry and geometry were confirmed by X-ray crystallography. Crystals suitable for single-crystal X-ray diffraction analysis were obtained for all the metal complexes by the layering of a methanolic solution of the pseudopeptidic ligand over a basic aqueous solution of Cu(OAc)$_2$ and Ni(OAc)$_2$. The X-ray crystal structures of the copper complexes **5a** and **6a** are presented in Fig. 5. X-ray diffraction data confirm the formation of the metal complexes with a 1 : 1 stoichiometry.

The Cu^{2+} cation in **5a** is coordinated by two amine groups and two deprotonated amide groups, in a distorted square-planar geometry, and displays a torsion angle of 13.8° between the N$_{amine}$–Cu–N$_{amide}$ planes. The Cu–N$_{amide}$ distances are slightly shorter than the Cu–N$_{amine}$ ones, being 1.921 and 2.052 Å on average, respectively.[7b] The N–Cu–N angles contained in the two five-membered rings N$_{amine}$–Cu–N$_{amide}$ are *ca.* 13° smaller than those contained in the N$_{amide}$–Cu–N$_{amide}$ six-membered ring, as expected for a smaller ring size with a tighter environment. The Cu^{2+} cation in **6a** is also coordinated by two amine groups and two deprotonated amide groups, in a distorted square-planar geometry, but displays a torsion angle of 29.9°. Again the Cu–N$_{amide}$ distances are slightly shorter than the ones for Cu–N$_{amine}$, being 1.912 and 2.034 Å on average, respectively, and both slightly shorter than in **5a**. The N–Cu–N angles contained in the two five-membered rings (N$_{amine}$–Cu–N$_{amide}$) are *ca.* 14° smaller than those in the six member ring (N$_{amide}$–Cu–N$_{amide}$).
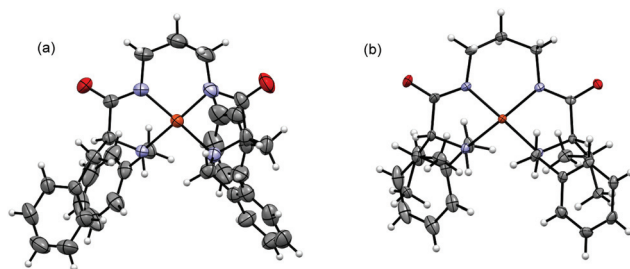

Fig. 5 X-ray crystal structures of Cu^{2+} complexes **5a** (a) and **6a** (b). Ellipsoids represented at the 50% probability level.
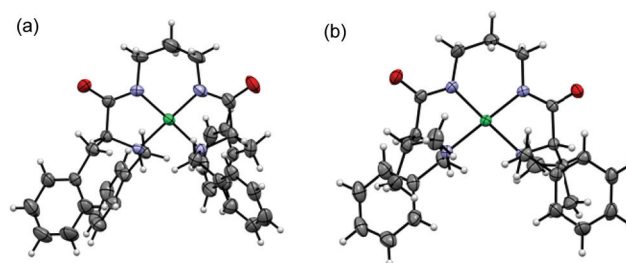

Fig. 6 X-ray crystal structure of complexes **5b** (a) and **6b** (b). Ellipsoids represented at the 50% probability level.

The X-ray crystal structures for the Ni^{2+} complexes **5b** and **6b** are presented in Fig. 6. Also for **5b** and **6b** the Ni^{2+} cation is coordinated by two amine groups and two deprotonated amide groups, in a distorted square-planar geometry displaying torsion angles of 12.9° and 14.8° respectively. In both complexes the Ni–N$_{amide}$ distances are slightly shorter than the corresponding Ni–N$_{amine}$ and the N–Ni–N angles contained in the five-membered rings are smaller than the angles contained in the six-membered ring (*ca.* 15° for **6b**).

Conclusions

N-Benzylation of the terminal amino nitrogen atoms in C_2-symmetric pseudopeptides containing an aliphatic central spacer provides significant changes in their properties as ligands. Thus, the solubility in water of **3** and **4** and that for their respective metal complexes decreases, in particular for the phenylalanine derivative (**3**), which precludes a more detailed analysis of its coordination chemistry. The corresponding spectroscopic, spectrometric and potentiometric studies could be carried out with the valine derivative **4**, in particular in aqueous mixed solvents, revealing that these bis(amino amides) are able to provide efficient tetradentate coordination for metal cations, in particular Cu^{2+}. The resulting Cu^{2+} and Ni^{2+} bisdeprotonated complexes seem to represent the most important complex species for both cations, even at slightly acidic pH regions at least for the system Cu^{2+}·**4**. The complexes display 1 : 1 stoichiometries and square planar arrangements around the metal centre, as suggested by spectroscopic data and confirmed by the corresponding X-ray structures. The presence of the additional benzyl groups in the terminal amino groups can significantly reduce the stability of the corresponding metal complexes, as has been observed when comparing the stability constants obtained potentiometrically for the system Cu^{2+}·**4** and those obtained for the non-benzylated analogue **2**. The observed decrease in the stability constants for Cu^{2+} is significantly higher than the one observed in the case of benzylated linear polyamines. This, however, facilitates the observation of a defined spectroscopic response to the interaction of **4** with Cu^{2+}, in particular at short times. It must be noted that the corresponding Cu^{2+} complexes display very strong bisigned CD signals that can be used advantageously to observe and characterize the formation

of such complexes, achieving LOD values of 28 µM while using UV-Vis measurements the value was 80–90 µM.

Experimental section

All reagents and solvents were obtained from commercial sources and used as received unless otherwise stated. Deionized water was used from a "Milli-Q® Integral Water Purification System" by Millipore. Microanalyses were performed on an elemental analyzer equipped with an oxygen module. Rotatory power was determined with a digital polarimeter (Na: 589 nm). Melting points were measured using a standard apparatus and are uncorrected.

General procedure for the synthesis of N,N′-benzylated bis(amino amides)

Compound 3. Compound **1** (3.01 g, 8.17 mmol) was dissolved in methanol (50 mL) and added to a solution of benzaldehyde (2.013 mL, 17.97 mmol) in methanol (10 mL) in a 100 mL two necked round bottom flask, under a nitrogen atmosphere. After stirring at room temperature for 3 h, the reaction mixture was treated with 50 mL of a methanolic solution of NaBH$_4$ (1.24 g, 32.68 mmol) and further stirred overnight. The solvent was evaporated and the crude product was dissolved in basic water (pH = 10–11) and extracted with CHCl$_3$ (3 × 50 mL). The organic phase was dried over anhydrous MgSO$_4$, and vacuum evaporated. The final pure product was obtained after washing with hexane as a white solid (3.418 g, 6.23 mmol, 76% Yield): mp 101–103 °C; $[\alpha]_D^{25}$ = −83.57 (c = 0.01, CHCl$_3$); IR (ATR) 3343, 3321, 2936, 1636, 1528, 1452 cm^{-1}; ^{1}H NMR (500 MHz, CDCl$_3$) δ 7.46 (t, J = 6.2 Hz, 2H), 7.24–7.13 (m, 7H), 7.09 (d, J = 7.0 Hz, 2H), 7.03 (d, J = 6.6 Hz, 2H), 3.66 (d, J = 13.4 Hz, 2H), 3.49 (d, J = 13.4 Hz, 2H), 3.31 (dd, J = 9.2, 4.4 Hz, 2H), 3.11 (dt, J = 15.3, 5.7 Hz, 4H), 2.69 (dd, J = 13.8, 9.3 Hz, 2H), 1.51–1.47 (m, 2H); ^{13}C NMR (126 MHz, CDCl$_3$) δ 173.3, 137.2, 129.2, 128.7, 128.5, 128.2, 127.4, 126.9, 63.1, 52.5, 39.0, 35.7, 29.8; HRMS (ESI-TOF)$^+$ Calcd for C$_{35}$H$_{41}$N$_4$O$_2$ (M + H)$^+$: 549.3230; found 549.3235; Anal. Calcd for C$_{35}$H$_{40}$N$_4$O$_2$: C, 76.6; H, 7.4; N, 10.2. Found: C, 76.2; H, 7.1; N, 10.0.

Compound 4. 2.380 g, 8.74 mmol, 87% Yield; mp 87–89 °C; $[\alpha]_D^{25}$ = −46.27 (c = 0.01, CHCl$_3$); IR (ATR) 3301, 2958, 2940, 2933, 2898, 2877, 1629, 1546 cm^{-1}; ^{1}H NMR (500 MHz, CDCl$_3$) δ 7.52 (s, 2H), 7.33 (s, 6H), 3.80 (d, J = 13.0 Hz, 2H), 3.66 (d, J = 13.1 Hz, 2H), 3.35–3.24 (m, 4H), 2.97 (d, J = 3.8 Hz, 2H), 2.12 (d, J = 5.6 Hz, 2H), 1.67–1.62 (m, 2H), 0.94 (dd, J = 29.5, 6.6 Hz, 12H); ^{13}C NMR (126 MHz, CDCl$_3$) δ 174.1, 139.8, 128.5, 128.2, 127.2, 77.3, 77.0, 76.77, 68.1, 53.5, 35.7, 31.4, 30.3, 19.7, 17.9; HRMS (ESI-TOF)$^+$ Calcd for C$_{27}$H$_{41}$N$_4$O$_2$ (M + H)$^+$: 453.3230, found 453.3227; Anal. Calcd for C$_{27}$H$_{40}$N$_4$O$_2$: C, 71.7; H, 8.9; N, 12.4. Found: C, 71.5; H, 8.7; N, 12.2.

General procedure for the synthesis of M^{2+} complexes

Compound **3** (100 mg, 0.182 mmol) was dissolved in dry MeOH (5 mL) in a 25 mL round bottom flask and maintained under a nitrogen atmosphere. Cu(OAc)$_2$ (36.38 mg,

0.182 mmol) dissolved in dry MeOH (5 mL) was then added and the mixture stirred for 30 min at room temperature. 1 M KOH in methanol (3.3 mL, 0.364 mmol) was added and the solution was maintained at room temperature overnight. The precipitate formed was filtered and washed with cold dichloromethane to afford the corresponding metal complex.

Complex 5a. 70.6 mg, 0.116 mmol, 64% Yield; FT-IR: 3500–3000, 2920, 1571, 1454, 1392 cm^{-1}; Anal. Calcd (%) for C$_{35}$H$_{38}$N$_4$O$_2$Cu·2H$_2$O: C, 65.1, H, 6.6, N, 8.7; found: C, 65.1, H, 6.5, N, 8.5.

Complex 5b. 73.5 mg, 0.121 mmol, 67% Yield; FT-IR: 3600–3000, 2931, 1573, 1452, 1398 cm^{-1}; Anal. Calcd (%) for C$_{35}$H$_{38}$N$_4$O$_2$Ni·2H$_2$O: C, 65.5, H, 6.6, N, 8.7; found: C, 65.4, H, 6.2, N, 8.6.

Complex 6a. 47.7 mg, 0.093 mmol, 42% Yield; FT-IR: 3600–3000, 1592, 1551, 1396 cm^{-1}; Anal. Calcd (%) for C$_{27}$H$_{38}$N$_4$O$_2$Cu·1.5H$_2$O: C, 59.9, H, 7.6, N, 10.4; found: C, 59.5, H, 7.4, N, 10.2.

Complex 6b. 51.2 mg, 0.101 mmol, 45.5% Yield; FT-IR: 3600–3000, 1649, 1569, 1453 cm^{-1}; Anal. Calcd (%) for C$_{27}$H$_{38}$N$_4$O$_2$Ni·3.5H$_2$O: C, 56.7, H, 7.9, N, 9.8; found: C, 56.3, H, 8.1, N, 9.7.

Electromotive force measurements

The potentiometric titrations were carried out at 298.1 K using 0.1 M NaCl as the supporting electrolyte. The experimental procedure (burette, potentiometer, cell, stirrer, microcomputer, *etc.*) has been fully described elsewhere.[34] The acquisition of the emf data was performed with the computer program CrisonCapture. The reference electrode was an Ag/AgCl electrode in saturated KCl solution. The glass electrode was calibrated as a hydrogen-ion concentration probe by titration of previously standardized amounts of HCl with CO$_2$-free NaOH solutions and the equivalence point determined by the Gran's method,[35] which gives the standard potential, $E^{0\prime}$, and the ionic product of water 13.78, whereas in the case of the H$_2$O/CH$_3$CN mixture used this value was 14.6.[15] The computer program HYPERQUAD was used to calculate the protonation and stability constants,[14] and the HySS29 program was used to obtain the distribution diagrams.[36] The pH range investigated was 2.0–12.0 and the concentration of the metal ions and the ligands 0.1 mM, with 1 : 1 M^{2+} : L molar ratios. The different titration curves for each system (at least two) were treated either as a single set or as separated curves without significant variations in the values of the stability constants. Finally, the sets of data were merged together and treated simultaneously to give the final stability constants.

^{1}H NMR experiments

The ^{1}H spectra were recorded on a Varian INOVA 500 spectrometer (500 and 125 MHz for ^{1}H and ^{13}C NMR, respectively). The solvent signal was used as a reference standard.

UV-Vis and CD measurements

UV-Vis absorption spectra were recorded using a Hewlett-Packard 8453 device. All measurements were performed at

room temperature and spectra were recorded from 200 to 900 nm. For metal titration experiments, a M^{2+} solution in MeOH/H_2O 80/20 (2.5 mM) and a solution of compound **4** (30 mM) in the same solvent mixture were used and aliquots of the ligand solution were gradually added to the metal solution using a micropipette. After equilibration, the corresponding absorptions were measured. For job-plot measurements stock solutions of compound **4** (5 mM in MeOH/H_2O 80/20) and Cu(OAc)$_2$ (5 mM in MeOH/H_2O 80/20) were prepared and mixed in variable proportions so that the final volume of the mixture was maintained constant to 1 mL. After equilibration, the absorbance at 490 nm of each solution was independently measured. A plot of absorbance against the mole fraction of Cu^{2+} was used to determine the metal–ligand ratio.

CD experiments were performed using a JASCO J-810 spectrometer. All measurements were performed at room temperature and spectra were recorded from 200 nm to 900 nm with 1.0 nm step and 1.0 nm bandwidth and the scanning speed was 200 nm per minute.

LOD values were calculated using the relation

$$\text{Detection limit} = 3\sigma/k$$

where σ is the standard deviation of the blank measurements,[32] and k is the slope between the absorbance for UV and mdeg for CD *versus* [L]. For such experiments, the UV-Vis and CD spectra of the solvent (blank) were measured 10 times and the standard deviation of the measurements was determined. The slope was obtained from the plot of absorbance at 490 nm for UV-Vis or from the amplitude of the Cotton effect ($\Delta CD = CD_{440nm} - CD_{520nm}$) *vs.* the concentration of ions.

Mass spectrometry

Mass spectra were recorded on a Q-TOF Premier mass spectrometer with an orthogonal Z-spray electrospray interface (Micromass, Manchester, UK) by electrospray positive mode (ES$^+$). The desolvation gas, as well as nebulizing gas, was nitrogen at a flow of 700 L h^{-1} and 20 L h^{-1}, respectively. The of the source block and desolvation temperatures were set to 120 °C and 150 °C. A capillary voltage of 3.5 kV was used in the positive scan mode, respectively. The cone voltage was typically set to 20 V to control the extent of fragmentation of the identified ions. Sample solutions were infused *via* syringe pump directly connected to the ESI source at a flow rate of 10 mL min^{-1}. The observed isotopic pattern of each intermediate perfectly matched the theoretical isotope pattern calculated from their elemental composition using the MassLynx 4.0 program.[37]

IR spectroscopy

FT-IR spectra were acquired on a JASCO 6200 equipment with a MIRacle single reflection ATR diamond/ZnSe accessory. The raw IR spectral data were processed with the JASCO spectral manager software.

Crystallography

Single crystals of ligand **4** and complexes **5a–6b** were obtained. A suitable crystal was selected and measured on a single crystal X-ray diffractometer. Using Olex2,[38] all the structures were solved with the ShelXS 2014 structure solution program using Direct Methods and refined with the ShelXL 2014 refinement package using Least Squares minimization.[39] The program MERCURY was used to prepare artwork representations.[40] Crystallographic data and refinement parameters are summarized in Table S1 (ESI†). Cambridge Crystallographic Data Centre files 1481178 (**3**), 1481179 (**5a**), 1481180 (**5b**), 1481181 (**6a**) and 1481182 (**6b**) contain the supplementary crystallographic data for this paper.

Notes and references

1 (*a*) W. Wang, Q. Wen, Y. Zhang, X. Fei, Y. Li, Q. Yang and X. Xu, *Dalton Trans.*, 2013, **42**, 1827–1833; (*b*) P. C. Dhar, A. Pal, P. Mohanty and B. Bag, *Sens. Actuators, B*, 2015, **219**, 308–314; (*c*) D. Singhal, N. Gupta and A. K. Singh, *RSC Adv.*, 2015, **5**, 65731–65738; (*d*) A. P. de Silva, H. Q. N. Gunaratne, T. Gunnlaugsson, A. J. M. Huxley, C. P. McCoy, J. T. Rademacher and T. E. Rice, *Chem. Rev.*, 1997, **97**, 1515–1566; (*e*) L. Pu, *Chem. Rev.*, 2004, **104**, 1687–1716; (*f*) G. W. Gokel, W. M. Leevy and M. E. Weber, *Chem. Rev.*, 2004, **104**, 2723–2750; (*g*) P. D. Beer and P. A. Gale, *Angew. Chem., Int. Ed.*, 2001, **40**, 486–516; (*h*) L. Prodi, F. Bolletta, M. Montalti and N. Zaccheroni, *Coord. Chem. Rev.*, 2000, **205**, 59–83; (*i*) V. Amendola, L. Fabbrizzi, F. Foti, M. Licchelli, C. Mangano, P. Pallavicini, A. Poggi, D. Sacchi and A. Taglietti, *Coord. Chem. Rev.*, 2006, **250**, 273–299.

2 (*a*) E. Gaggelli, H. Kozlowski, D. Valensin and G. Valensin, *Chem. Rev.*, 2006, **106**, 1995–2044; (*b*) A. Mathie, G. L. Sutton, C. E. Clarke and E. L. Veale, *Pharmacol. Ther.*, 2006, **111**, 567–583; (*c*) K. J. Barnham, C. L. Masters and A. I. Bush, *Nat. Rev. Drug Discovery*, 2004, **3**, 205–214; (*d*) D. J. Waggoner, T. B. Bartnikas and J. D. Gitlin, *Neurobiol. Dis.*, 1999, **6**, 221–230; (*e*) L. I. Bruijn, T. M. Miller and D. W. Cleveland, *Annu. Rev. Neurosci.*, 2004, **27**, 723–749; (*f*) C. Zhao, B. Liu, X. Bi, D. Liu, C. Pan, L. Wang and Y. Pang, *Sens. Actuators, B*, 2016, **229**, 131–137.

3 (*a*) Y. Xiang, Z. Li, X. Chen and A. Tong, *Talanta*, 2008, **74**, 1148–1153; (*b*) B. High, D. Bruce and M. M. Richter, *Anal. Chim. Acta*, 2001, **449**, 17–22; (*c*) L. Tapia, M. Suazo, C. Hödar, V. Cambiazo and M. González, *BioMetals*, 2003, **16**, 169–174; (*d*) F. Chen, G. Liu, Y. Shi, P. Xi, J. Cheng, J. Hong, R. Shen, X. Yao, D. Bai and Z. Zeng, *Talanta*, 2014,

124, 139–145; (*e*) D. Zha and L. You, *ACS Appl. Mater. Interfaces*, 2016, **8**, 2399–2405.

4 (*a*) B. Valeur and I. Leray, *Coord. Chem. Rev.*, 2000, **205**, 3–40; (*b*) N. Kaur and S. Kumar, *Tetrahedron*, 2011, **67**, 9233–9264.

5 (*a*) L. Fabbrizzi and A. Poggi, *Chem. Soc. Rev.*, 2013, **42**, 1681–1699; (*b*) A. E. Martell, R. M. Smith and R. M. Moteikaitis, *NIST Critical Stability Constants Database*, Texas A&M University, College Station, TX, 1993.

6 (*a*) B. Dangel, M. Clarke, J. Haley, D. Sames and R. Polt, *J. Am. Chem. Soc.*, 1997, **119**, 10865–10866; (*b*) B. D. Dangel and R. Polt, *Org. Lett.*, 2000, **2**, 3003–3006; (*c*) R. Polt, B. D. Kelly, B. D. Dangel, U. B. Tadikonda, R. E. Ross, A. M. Raitsimring and A. V. Astashkin, *Inorg. Chem.*, 2003, **42**, 566–574; (*d*) M. Merschky and C. Schmuck, *Org. Biomol. Chem.*, 2009, **7**, 4895–4903; (*e*) Ł. Weseliński, E. Słyk and J. Jurczak, *Tetrahedron Lett.*, 2011, **52**, 381–384; (*f*) J. Paradowska, M. Pasternak, B. Gut, B. Gryzło and J. Mlynarski, *J. Org. Chem.*, 2012, **77**, 173–187; (*g*) F. Adrián, M. I. Burguete, J. M. Fraile, J. I. García, J. García, E. García-España, S. V. Luis, J. A. Mayoral, A. J. Royo and M. C. Sánchez, *Eur. J. Inorg. Chem.*, 1999, 2347–2354; (*h*) R. R. Wagler, Y. Fang and C. J. Burrows, *J. Org. Chem.*, 1989, **54**, 1584–1589.

7 (*a*) S. Blasco, M. I. Burguete, M. P. Clares, E. García-España, J. Escorihuela and S. V. Luis, *Inorg. Chem.*, 2010, **49**, 7841–7852; (*b*) I. Martí, A. Ferrer, J. Escorihuela, M. I. Burguete and S. V. Luis, *Dalton Trans.*, 2012, **41**, 6764–6776; (*c*) V. Martí-Centelles, D. K. Kumar, A. J. P. White, S. V. Luis and R. Vilar, *CrystEngComm*, 2011, **13**, 6997–7008; (*d*) L. Gorla, V. Martí-Centelles, B. Altava, M. I. Burguete and S. V. Luis, *Inorg. Chem.*, 2016, **55**, 7617–7629.

8 E. Faggi, R. Gavara, M. Bolte, L. Fajari, L. Julia, L. Rodriguez and I. Alfonso, *Dalton Trans.*, 2015, **44**, 12700–12710.

9 J. Becerril, M. Bolte, M. I. Burguete, F. Galindo, E. García-España, S. V. Luis and J. F. Miravet, *J. Am. Chem. Soc.*, 2003, **125**, 6677–6686.

10 (*a*) I. Alfonso, M. Bolte, M. Bru, M. I. Burguete, S. V. Luis and J. Rubio, *J. Am. Chem. Soc.*, 2008, **130**, 6137–6144; (*b*) M. Bru, I. Alfonso, M. Bolte, M. I. Burguete and S. V. Luis, *Chem. Commun.*, 2011, **47**, 283–285.

11 (*a*) I. Alfonso, M. I. Burguete and S. V. Luis, *J. Org. Chem.*, 2006, **71**, 2242–2250; (*b*) I. Alfonso, M. I. Burguete, F. Galindo, S. V. Luis and L. Vigara, *J. Org. Chem.*, 2007, **72**, 7947–7956; (*c*) E. Faggi, S. V. Luis and I. Alfonso, *RSC Adv.*, 2013, **3**, 11556–11565.

12 (*a*) A. E. Martell and R. J. Motekaitis, *Coord. Chem. Rev.*, 1990, **100**, 323–361; (*b*) A. Bencini, A. Blanchi, E. Garcia-España, M. Micheloni and J. A. Ramirez, *Coord. Chem. Rev.*, 1999, **188**, 97–156.

13 (*a*) E. García-España, P. Díaz, J. M. Llinares and A. Bianchi, *Coord. Chem. Rev.*, 2006, **250**, 2952–2986; (*b*) A. Bianchi, B. Escuder, E. García-España, S. V. Luis, V. Marcelino, J. F. Miravet and J. A. Ramírez, *J. Chem. Soc., Perkin Trans. 2*, 1994, 1253–1259; (*c*) V. J. Arán, M. Kumar, J. Molina, L. Lamarque, P. Navarro, E. García-España, J. A. Ramírez, S. V. Luis and B. Escuder, *J. Org. Chem.*, 1999, **64**, 6135–6146; (*d*) J. A. Aguilar, E. García-España, J. Guerrero, S. V. Luis, J. Llinares, J. Ramírez and C. Soriano, *Inorg. Chim. Acta*, 1996, **246**, 287–294; (*e*) A. Bencini, A. Bianchi, M. I. Burguete, P. Dappporto, A. Doménech, E. García-España, S. V. Luis, P. Paoli and J. A. Ramírez, *J. Chem. Soc., Perkin Trans. 2*, 1994, 569–577; (*f*) M. T. Albelda, M. A. Bernardo, E. García-España, M. L. Godino-Salido, S. V. Luis, M. J. Melo, F. Pina and C. Soriano, *J. Chem. Soc., Perkin Trans. 2*, 1999, 2545–2549; (*g*) G. Nishimura, K. Ishizumi, Y. Shiraishi and T. Hirai, *J. Phys. Chem. B*, 2006, **110**, 21596–21602.

14 P. Gans, A. Sabatini and A. Vacca, *Talanta*, 1996, **43**, 1739–1753.

15 M. A. Herrador and A. G. González, *Talanta*, 2002, **56**, 769–775.

16 (*a*) B. Dietrich, M. W. Hosseini, J.-M. Lehn and R. B. Sessions, *Helv. Chim. Acta*, 1983, **66**, 1262–1278; (*b*) M. W. Hosseini and J. M. Lehn, *J. Am. Chem. Soc.*, 1982, **104**, 3525–3527; (*c*) M. W. Hosseini and J. M. Lehn, *Helv. Chim. Acta*, 1986, **69**, 587–603; (*d*) B. Dietrich, M. W. Hosseini, J. M. Lehn and R. B. Sessions, *J. Am. Chem. Soc.*, 1981, **103**, 1282–1283; (*e*) A. Bencini, A. Bianchi, E. Garcia-España, M. Giusti, M. Micheloni and P. Paoletti, *Inorg. Chem.*, 1987, **26**, 681–684; (*f*) A. Bencini, A. Bianchi, E. Garcia-España, M. Micheloni and P. Paoletti, *Inorg. Chem.*, 1988, **27**, 176–180.

17 P. Seliger, D. Tomczyk, G. Andrijewski and E. Tomal, *J. Anal. Methods Chem.*, 2016, **2016**, 1721069.

18 D. B. Rorabacher, W. J. MacKellar, F. R. Shu and S. M. Bonavita, *Anal. Chem.*, 1971, **43**, 561–573.

19 (*a*) S. H. Gellman, G. P. Dado, C.-B. Liang and B. R. Adam, *J. Am. Chem. Soc.*, 1991, **113**, 1164–1173; (*b*) T. Schneider, K. T. Halloran, J. A. Hillner, R. R. Conry and B. R. Linton, *Chem. – Eur. J.*, 2013, **19**, 15101–15104; (*c*) A. Mazzanti, M. Chiarucci, L. Prati, K. W. Bentley and C. Wolf, *J. Org. Chem.*, 2016, **81**, 89–99.

20 (*a*) C. A. Hunter and H. L. Anderson, *Angew. Chem., Int. Ed.*, 2009, **48**, 7488–7499; (*b*) A. S. Mahadevi and G. N. Sastry, *Chem. Rev.*, 2016, **116**, 2775–2825.

21 (*a*) J. Rebek, T. Costello, L. Marshall, R. Wattley, R. C. Gadwood and K. Onan, *J. Am. Chem. Soc.*, 1985, **107**, 7481–7487; (*b*) J. Rebek, *Acc. Chem. Res.*, 1984, **17**, 258–264; (*c*) F. Gaviña, S. V. Luis, A. M. Costero, M. I. Burguete and J. Rebek, *J. Am. Chem. Soc.*, 1988, **110**, 7140–7143.

22 E. N. W. Howe, M. Bhadbhade and P. Thordarson, *J. Am. Chem. Soc.*, 2014, **136**, 7505–7516.

23 (*a*) The colourless H_2O/MeOH solution of **4** did not absorb in the visible-UV region from 350 to 800 nm; (*b*) O. Horvath and K. L. Stevenson, *Charge-transfer photochemistry of coordination compounds*, VCH, Weinheim, Germany, 1993; (*c*) M. A. Bernardo, F. Pina, E. García-España, J. Latorre, S. V. Luis, J. M. Llinares, J. A. Ramírez and C. Soriano, *Inorg. Chem.*, 1998, **37**, 3935–3942.

24 (a) M. A. Pauly, E. M. Erwin, D. R. Powell, G. T. Rowe and L. Yang, *Polyhedron*, 2015, **102**, 722–734; (b) W. Wang, Y. A. Lee, G. Kim, S. K. Kim, G. Y. Lee, J. Kim, Y. Kim, G. J. Park and C. Kim, *J. Inorg. Biochem.*, 2015, **153**, 143–149; (c) P. D. Wadhavane, L. Gorla, A. Ferrer, B. Altava, M. I. Burguete, M. A. Izquierdo and S. V. Luis, *RSC Adv.*, 2015, **5**, 72579–72589.

25 (a) F. A. Cotton, G. Wilkinson, C. A. Murillo and M. Bochmann, *Advanced Inorganic Chemistry*, Wiley, New York, 6th edn, 1999; (b) G. Bussière and C. Reber, *J. Am. Chem. Soc.*, 1998, **120**, 6306–6315; (c) W. Liu, A. Migdisov and A. Williams-Jones, *Geochim. Cosmochim. Acta*, 2012, **94**, 276–290.

26 (a) M. Rajasekar, S. Sreedaran, R. Prabu, V. Narayanan, R. Jegadeesh, N. Raaman and A. K. Rahiman, *J. Coord. Chem.*, 2010, **63**, 136–146; (b) J. Manonmani, R. Thirumuruhan, M. Kandaswamy, V. Narayanan, S. S. S. Raj, M. N. Ponnuswamy, G. Shanmugam and H. K. Fun, *Polyhedron*, 2001, **20**, 3039–3048.

27 (a) M. G. Basallote, M. J. Fernandez-Trujillo and M. A. Manez, *J. Chem. Soc., Dalton Trans.*, 2002, 3691–3695; (b) F. T. R. D. Almeida, B. C. S. Ferreira, A. L. D. S. L. Moreira, R. P. D. Freitas, L. F. Gil and L. V. A. Gurgel, *J. Colloid Interface Sci.*, 2016, **466**, 297–309.

28 (a) P. Job, *Anal. Chim. Appl.*, 1928, **9**, 113–203; (b) H.-J. Schneider and A. Yatsimirsky, *Principles and Methods in Supramolecular Chemistry*, John Wiley & Sons, Chichester, 2000; (c) P. Thordarson, *Chem. Soc. Rev.*, 2011, **40**, 1305–1323; (d) J. S. Renny, L. L. Tomasevich, E. H. Tallmadge and D. B. Collum, *Angew. Chem., Int. Ed.*, 2013, **52**, 11998–12013.

29 For limitations of the Job plot, in particular for weak supramolecular complexes, see, for instance: (a) F. Ulatowski, K. Dąbrowa, T. Bałakier and J. Jurczak, *J. Org. Chem.*, 2016, **81**, 1746–1756; (b) D. B. Hibberta and P. Thordarson, *Chem. Commun.*, 2016, **52**, 12792–12805.

30 (a) S. K. Sharma, G. Hundal and R. Gupta, *Eur. J. Inorg. Chem.*, 2010, **2010**, 621–636; (b) S. Kumar and R. Gupta, *Indian J. Chem., Sect. A: Inorg., Bio-inorg., Phys., Theor. Anal. Chem.*, 2011, **50**, 1369–1379; (c) N. Tounsi, L. Dupont, A. Mohamadou, E. Guillon, M. Aplincourt and G. Rogez, *Polyhedron*, 2008, **27**, 3674–3682; (d) L.-M. López-Martínez, H. Santacruz-Ortega, R. E. Navarro, L. Machi-Lara, R. Sugich-Miranda and K. Ochoa-Lara, *Polyhedron*, 2014, **79**, 338–346.

31 (a) S.-P. Wu, K.-J. Du and Y.-M. Sung, *Dalton Trans.*, 2010, **39**, 4363–4368; (b) C. Liu, J. Xu, F. Yang, W. Zhou, Z. Li, L. Wei and M. Yu, *Sens. Actuators, B*, 2015, **212**, 364–370; (c) Y. Wang, C. Wang, S. Xue, Q. Liang, Z. Li and S. Xu, *RSC Adv.*, 2016, **6**, 6540–6550; (d) R. V. Rathod, S. Bera, M. Singh and D. Mondal, *RSC Adv.*, 2016, **6**, 34608–34615; (e) J.-J. Xiong, P.-C. Huang, C.-Y. Zhang and F.-Y. Wu, *Sens. Actuators, B*, 2016, **226**, 30–36; (f) Y. Ma, T. Leng, Y. Qu, C. Wang, Y. Shen and W. Zhu, *Tetrahedron*, 2017, **73**, 14–20.

32 (a) F. L. Capitán-Vallvey, E. Arroyo-Guerrero, D. M. Fernández-Ramos and F. Santoyo-González, *Microchim. Acta*, 2005, **151**, 93–100; (b) IUPAC. Compendium of Chemical Terminology, 2nd ed. (the "Gold Book"). Compiled by A. D. McNaught and A. Wilkinson, Blackwell Scientific Publications, Oxford (1997). XML online corrected version: http://goldbook.iupac.org (2006) created by M. Nic, J. Jirat, B. Kosata; updates compiled by A. Jenkins. ISBN 0-9678550-9-8.

33 X. Wu, L. Xu, L. Liu, W. Ma, H. Yin, H. Kuang, L. Wang, C. Xu and N. A. Kotov, *J. Am. Chem. Soc.*, 2013, **135**, 18629–18636.

34 E. Garcia-España, M.-J. Ballester, F. Lloret, J. M. Moratal, J. Faus and A. Bianchi, *J. Chem. Soc., Dalton Trans.*, 1988, 101–104.

35 (a) G. Gran, *Analyst*, 1952, **77**, 661–671; (b) F. J. C. Rossotti and H. Rossotti, *J. Chem. Educ.*, 1965, **42**, 375.

36 L. Alderighi, P. Gans, A. Ienco, D. Peters, A. Sabatini and A. Vacca, *Coord. Chem. Rev.*, 1999, **184**, 311–318.

37 (a) *MassLynx Software, version 4.0*; (b) S. Moco, R. J. Bino, O. Vorst, H. A. Verhoeven, J. de Groot, T. A. van Beek, J. Vervoort and C. H. R. de Vos, *Plant Physiol.*, 2006, **141**, 1205–1218.

38 O. V. Dolomanov, L. J. Bourhis, R. J. Gildea, J. A. K. Howard and H. Puschmann, *J. Appl. Crystallogr.*, 2009, **42**, 339–341.

39 G. Sheldrick, *Acta Crystallogr.*, 2008, **64**, 112–122.

40 C. F. Macrae, I. J. Bruno, J. A. Chisholm, P. R. Edgington, P. McCabe, E. Pidcock, L. Rodriguez-Monge, R. Taylor, J. van de Streek and P. A. Wood, *J. Appl. Crystallogr.*, 2008, **41**, 466–470.